Biochemistry and Biophysics Reports 11 (2017) 72–78

Contents lists available at ScienceDirect

Biochemistry and Biophysics Reports

journal homepage: www.elsevier.com/locate/bbrep

Pentylenetetrazol modulates redox system by inducing addicsin translocation from endoplasmic reticulum to plasma membrane in NG108-15 cells

Mitsushi J. Ikemoto[a,b,*], Yusuke Murasawa[c], Pi-Chao Wang[d,**]

[a] Biomedical Research Institute, National Institute of Advanced Industrial Science and Technology (AIST), Tsukuba Central 6, 1-1-1 Higashi, Tsukuba, Ibaraki 305-8566, Japan
[b] Graduate School of Science, Toho University, 2-2-1 Miyama, Funabashi, Chiba 274-8510, Japan
[c] National Center for Geriatrics and Gerontology, 7-430 Morioka, Obu, Aichi 474-851, Japan
[d] Graduate School of Life and Environmental Sciences, University of Tsukuba, 1-1-1 Tennodai, Tsukuba, Ibaraki 305-8572, Japan

ARTICLE INFO

Keywords:
Addicsin (Arl6ip5/GTRAP3-18/JWA/PRAF3)
Pentylenetetrazol
Translocation
Plasma membrane
Cytotoxicity
Radical-scavenging activity

ABSTRACT

Addicsin (Arl6ip5) is a multifunctional physiological and pathophysiological regulator that exerts its effects by readily forming homo- and hetero-complexes with various functional factors. In particular, addicsin acts as a negative modulator of neural glutamate transporter excitatory amino acid carrier 1 (EAAC1) and participates in the regulation of intracellular glutathione (GSH) content by negatively modulating EAAC1-mediated cysteine and glutamate uptake. Addicsin is considered to play a crucial role in the onset of neurodegenerative diseases including epilepsy. However, the molecular dynamics of addicsin remains largely unknown. Here, we report the dynamics of addicsin in NG108-15 cells upon exposure to pentylenetetrazol (PTZ), a representative epileptogenic agent acting on the gamma-Aminobutyric acid A ($GABA_A$) receptor. Fluorescent immunostaining analysis demonstrated that addicsin drastically changed its localization from the endoplasmic reticulum (ER) to the plasma membrane within 1 h of PTZ exposure in a dose-dependent manner. Moreover, addicsin was co-localized with the plasma membrane markers EAAC1 and Na^+/K^+ ATPase alpha-3 upon PTZ stimulation. This translocation was significantly inhibited by a non-competitive $GABA_A$ receptor antagonist, picrotoxin, but not by a competitive $GABA_A$ receptor antagonist, bicuculline. Furthermore, lactate dehydrogenase (LDH) assay and 2,2-diphenyl-1-picrylhydrazyl (DPPH) radical-scavenging assay showed that PTZ-induced addicsin translocation was accompanied by a decrease of radical-scavenging activity and an increase of cytotoxicity in a PTZ dose-dependent manner. These findings suggest that PTZ induces the translocation of addicsin from the ER to the plasma membrane and modulates the redox system by regulating EAAC1-mediated GSH synthesis, which leads to the activation of cell death signaling.

1. Introduction

Addicsin has been identified as a novel factor encoding a 23-kDa hydrophobic protein that is highly upregulated in the amygdala nuclei of chronically morphine-administered mice [1,2]. It is also known as ADP-ribosylation-like factor 6 interacting protein 5 (Arl6ip5) and is the murine homolog of human JWA, rat glutamate transporter-associated protein 3–18 (GTRAP3-18), and PRA1 domain family member 3 (PRAF3) [3]. Addicsin is a multifunctional physiological and pathophysiological regulator that acts by easily forming homo- and hetero-complexes with many factors, including neural glutamate transporter excitatory amino acid carrier 1 (EAAC1), a neural glutamate transporter, addicsin itself, ADP-ribosylation-like factor 6-interacting protein 1 (Arl6ip1/ARMER), an apoptosis regulatory factor, and tomoregulin-1 (TMEFF1), an EGF-like domain-containing receptor [3–6]. To understand the diverse physiological functions of addicsin, it is essential to

Abbreviations: Arl6ip1/ARMER, ADP-ribosylation-like factor 6- interacting protein 1; ANOVA, analysis of variance; DPPH, 2,2-diphenyl-1-picrylhydrazyl; DMEM, Dulbecco's Modified Eagle Medium; EEAC1, excitatory amino acid carrier 1; TMEFF1, tomoregulin-1; ER, endoplasmic reticulum; GABA, gamma-Aminobutyric acid; GAPDH, glyceraldehyde 3-phosphate dehydrogenase; GSH, glutathione; IC, immunocytochemistry; IgG, immunoglobulin G; LDH, lactate dehydrogenase; PBS, phosphate-buffered saline; PCR, polymerase chain reaction; PTZ, pentylenetetrazol; PVDF, polyvinylidene fluoride; RT, room temperature; SDS, sodium dodecyl sulfate; WB, western blotting

* Corresponding author at: Biomedical Research Institute, National Institute of Advanced Industrial Science and Technology (AIST), Tsukuba Central 6, 1-1-1 Higashi, Tsukuba, Ibaraki 305-8566, Japan.
** Corresponding author.
E-mail addresses: m.ikemoto@aist.go.jp (M.J. Ikemoto), wangpicao@gmail.com (P.-C. Wang).

http://dx.doi.org/10.1016/j.bbrep.2017.06.008
Received 24 March 2017; Received in revised form 9 June 2017; Accepted 22 June 2017
Available online 27 June 2017

describe more precisely the addicsin-complex network and its dynamic regulation [3].

Low glutathione (GSH) content contributes to the development of neurodegenerative disorders including Alzheimer's disease and Parkinson's disease, as well as epilepsy [7]. Recent studies have strongly suggested that addicsin participates in the development of neurodegenerative disorders because it regulates neural GSH synthesis by negatively modulating EAAC1-mediated cysteine and glutamate uptake as GSH is synthesized from cysteine and glutamate [8,9]. In epilepsy, addicsin knockdown was found to decrease the seizure threshold and to accelerate kindling by the promotion of (gamma-Aminobutyric acid) GABA synthesis in rat hippocampal formation [10]. In a pentylenetetrazol (PTZ)-induced kindled rat model, addicsin expression was suppressed in the central nervous system [11]. Furthermore, EAAC1 knockdown produced mild neurotoxicity and epilepsy mediated by the decrease in GABA synthesis as EAAC1 is localized to the GABAergic inhibitory neurons to regulate GABA synthesis through the uptake of its precursor glutamate [11,12]. However, there is a lack of even basic information on the dynamics of addicsin in epilepsy.

Here, to shed light on this issue, we investigated the PTZ-induced dynamics of the expression and localization of addicsin in NG108-15 cells using immunocytochemical and cell biological analyses. We showed that addicsin changed its localization from the ER to the plasma membrane upon exposure to PTZ via $GABA_A$-mediated cell signaling. Furthermore, we revealed that this PTZ-induced change of addicsin localization leads to a decrease of radical-scavenging activity and an increase of cytotoxicity.

2. Materials and methods

2.1. Materials

The following materials were used in this study: Dulbecco's Modified Eagle Medium (DMEM) from Sigma-Aldrich (St. Louis, MO, USA); fetal bovine serum (FBS), TRIzol reagent, SuperScript II reverse transcriptase, and AmpliTaq Gold 360 Master Mix from Thermo Fisher Scientific Inc. (Waltham, MA, USA); picrotoxin, (−)-bicuculline methochloride, and the LDH-Cytotoxic Test *Wako* for Cytotoxicity from Wako Pure Chemical Industries, Ltd. (Osaka, Japan); pentylenetetrazol (PTZ) from MP Biomedicals, LLC (Santa Ana, CA, USA); 1,2-diphenyl-2-picrylhydrazyl (DPPH) from Cayman Chemical Company (Ann Arbor, MI, USA); Clarity™ Western ECL substrate and polyvinylidene fluoride (PVDF) membrane from Bio-Rad (Hercules, CA, USA); polyclonal rabbit anti-addicsin immunoglobulin G (IgG) antibody [1.3 mg/ml, 1:200 dilution for Western blotting (WB), 1:100 dilution for immunocytochemistry (IC)] from Transgenic Co. Ltd. (Kumamoto, Japan); polyclonal goat anti-Arl6ip1 (ARMER C-12) IgG antibody (0.2 mg/ml, 1:100 dilution for IC) and monoclonal mouse anti-EAAC1 (EAT3C-20) IgG (0.2 mg/ml, 1:100 dilution for IC) from Santa Cruz Biotechnologies (Santa Cruz, CA, USA); monoclonal mouse anti-actin IgG (1.0 mg/ml, 1:400 dilution for WB) from Sigma-Aldrich; monoclonal mouse anti-Na^+/K^+ATPase alpha-3 IgG antibody (1.0 mg/ml, 1:200 dilution for IC) and Alexa Fluor 568-conjugated donkey anti-rabbit IgG (2.0 mg/ml, 1:400 dilution for IC) from Thermo Fisher Scientific Inc.; peroxidase-conjugated goat anti-rabbit IgG (1.7 mg/ml, 1:2000 dilution for WB) from Cappel (Durham, NC, USA); FITC-conjugated donkey anti-rabbit IgG (1.5 mg/ml, 1:500 dilution for IC) from Jackson ImmunoResearch (West Grove, PA, USA); rhodamine-conjugated donkey anti-mouse IgG (1.0 mg/ml, 1:500 dilution for IC) from Chemicon International (Temecula, CA, USA); FITC-conjugated donkey anti-goat IgG (1.0 mg/ml, 1:400 dilution for IC), and Texas Red-conjugated donkey anti-goat IgG (1.0 mg/ml, 1:500 dilution for IC) from Rockland (Gilbertsville, PA, USA); and Alexa Fluor 488-conjugated donkey anti-goat IgG (2.0 mg/ml, 1:400 dilution for IC) from Abcam (Cambridge Science Park, Cambridge, UK).

2.2. Cell culture

NG108-15 cells (rodent neural hybrid cells) and 293 T cells (human embryonic kidney cells) were maintained in high-glucose DMEM supplemented with 10% FBS (10% FBS-DMEM) at 37 °C in a humidified 5% CO_2 incubator. In LDH and DPPH radical-scavenging assays, NG108-15 cells were cultured with 100 µl/well of 10% FBS-DMEM in a 96-well plate (Falcon) until 80–90% confluence. The dose of PTZ used in this study was based on the information described in the previous paper [13].

2.3. Reverse transcription polymerase chain reaction analysis

Single-stranded cDNA was synthesized using SuperScript II reverse transcriptase from total RNAs prepared from cells using TRIzol™ reagent. Polymerase chain reaction (PCR) was carried out using specific primers for the target cDNA with AmpliTaq Gold 360 Master Mix. Amplification entailed 35 cycles after pretreatment at 95 °C for 30 s using the following schedule: 95 °C for 30 s, 52 °C for 20 s, and 72 °C for 45 s. The primers for addicsin (496 bp) were 5′-TGC CTG GGA CGA TTT CTT CC-3′ and 5′-ATC TTC CTG CTG TTC CAA GG-3′. The primers for glyceraldehyde 3-phosphate dehydrogenase (GAPDH) (434 bp) were 5′-GTG GCA GTG ATG GCA TGG ACT-3′ and 5′-TTC ATT GAC CTC AAC TAC ATG-3′.

2.4. Western blot analysis

Western blot analysis was performed as previously described [5]. In brief, whole-cell lysates were prepared by dissolving in 200 µl of sodium dodecyl sulfate (SDS) sample buffer (62.5 mM Tris-HCl pH 6.8, 20% glycerol, 2% SDS, 0.005% bromophenol blue). The whole-cell lysates (15 µl) were subjected to 12% SDS-PAGE and then transferred to a PVDF membrane. After the blots had been blocked with 10% dried milk in PBS containing 0.1% Tween-20 (PBS-T), they were incubated with specific antibodies for the target proteins. After incubation with HRP-conjugated secondary antibody, specific signals were detected by using the Clarity™ Western ECL substrate.

2.5. Immunocytochemical analysis

Double immunocytochemical analysis was performed to analyze the localization of endogenous addicsin and Arl6ip1 in NG108-15 cells, in accordance with previously described procedures [6]. The cultured NG108-15 cells treated with or without 20 mM PTZ for 24 h were fixed with PBS containing 4% paraformaldehyde at room temperature (R.T.) for 15 min. The cells were blocked with PBS containing 5% donkey serum at R.T. for 30 min, and were then reacted overnight at 4 °C with first the primary antibody and then the secondary antibody. The combination of rabbit anti-addicsin IgG with FITC-conjugated donkey anti-rabbit IgG was used to obtain the results shown in Figs. 1, 2B, and 3. Combinations of goat anti-Arl6ip1 IgG with FITC-conjugated donkey anti-goat IgG and of rabbit anti-addicsin IgG with Alexa Fluor 588-conjugated donkey anti-rabbit IgG were used for the results in Fig. 2A. The matching of mouse anti-EAAC1 IgG and Rhodamine-conjugated donkey anti-mouse IgG, and that of mouse anti-Na^+/K^+ATPase alpha-3 IgG antibody with Rhodamine-conjugated donkey anti-mouse IgG were employed for Fig. 2B. The combination of goat anti-Arl6ip1 IgG with Texas Red-conjugated donkey anti-goat IgG was used for Fig. 3. Fluorescent images in Figs. 1 and 2 were acquired using a Fluoview FV1000 confocal laser-scanning microscope (Olympus, Tokyo, Japan) and those in Fig. 3 were obtained using a BZ-X710 microscope (Keyence, Tokyo, Japan).

2.6. DPPH radical scavenging assay

DPPH radical scavenging assay was carried out as described

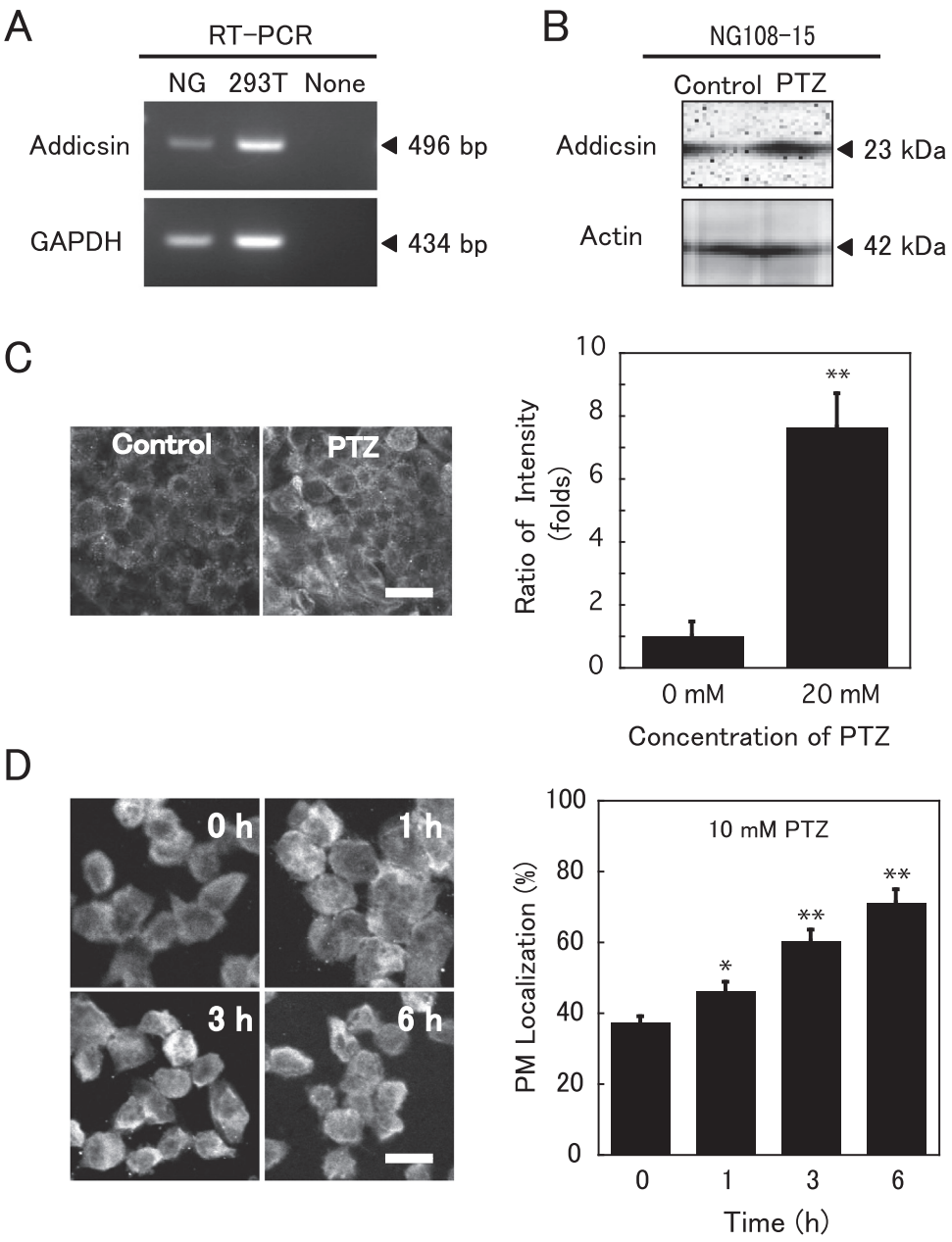

Fig. 1. Expression profile of addicsin in NG108-15 cells. (A) Expression of addicsin mRNA in NG108-15 cells. Mammalian addicsin mRNA and GAPDH mRNA prepared from NG108-15 cells or 293 T cells were analyzed by RT-PCR. The GAPDH transcript was detected as a positive control. (B) Expression of addicsin protein in NG108-15 cells. Expression of addicsin protein was investigated using whole NG108-15 cell lysates treated with or without exposure to 20 mM PTZ for 24 h by western blot analysis. (C) Expression level and localization of addicsin protein in NG108-15 cells. The cells treated with or without 20 mM PTZ for 24 h were examined by fluorescent immunostaining using anti-addicsin antibody (right panel). The fluorescent intensity of addicsin-IR-positive cells was determined by Image J software (left panel). Data are mean ± S.E.M, $n = 3$; **, t-test; $p < 0.01$. (D) Time course of addicsin localization pattern. After cells had been stained with anti-addicsin antibody at 0, 1, 3, or 6 h after 10 mM PTZ exposure, the stained cells were randomly photographed three times under each condition. The proportion of cells in which addicsin localized at the plasma membrane was determined by counting the total numbers of cells in which addicsin was or was not mainly localized at the plasma membrane from photographs taken in three independent experiments. Data are mean ± S.E.M, n = 3; $F_{4,11} = 29.16$, $p < 0.001$; one-way ANOVA. *, $p < 0.05$ vs. Control (0 h) group; **, $p < 0.01$ vs. Control (0 h) group. Scale bar corresponds to 40 μm in (C) and 25 μm in (D).

previously [14]. In brief, after cells had been pre-incubated with various concentrations of PTZ (0, 20, or 40 mM) or picrotoxin (0, 100, or 200 μM), a $GABA_A$ antagonist, for 24 h at 37 °C under 5% CO_2, 50 μl of culture medium was transferred into each well of a new 96-well plate and mixed with 50 μl of 0.2 mM DPPH. This mixture was then incubated at R.T. for 30 min in the dark. Radical-scavenging activity in each sample was evaluated by measuring the absorbance at 570 nm using a Model 680 Microplate Reader (Bio-Rad). The experimental data were obtained in duplicate.

2.7. LDH assay

The LDH assay was performed in accordance with the manufacturer's protocol. In brief, the cells were pre-incubated with various concentrations of PTZ (0, 5, 10, 20, or 40 mM) or picrotoxin (0, 100, or 200 μM), a non-competitive $GABA_A$ antagonist, for 24 h at 37 °C under 5% CO_2. After 24 h, the assay was carried out using 50 μl of culture medium in each well. Cytotoxicity in each sample was evaluated by determining the absorbance at 570 nm using a Model 680 Microplate Reader (Bio-Rad). The experimental data were acquired in duplicate.

2.8. Image analysis

Each two-gradation image was produced from a photograph taken upon fluorescent immunostaining using Adobe Photoshop CS3 Extended software (Ver. 10.0.1) (Adobe Systems Inc., San Jose, CA, USA). The subtracted images were obtained by correction based on the brightness of control cells. They were used to analyze the intensity and cell numbers using Image J Ver. 1.48 (NIH) [15].

2.9. Statistical analysis

All data are presented as the means ± S.E.M. of at least three independent experiments. One-way analysis of variance (ANOVA) test was performed to compare differences upon multiple comparisons using KaleidaGraph Ver. 4.50 software (Synergy Software, Reading, PA, USA). Differences were considered to be statistically significant at $p < 0.05$.

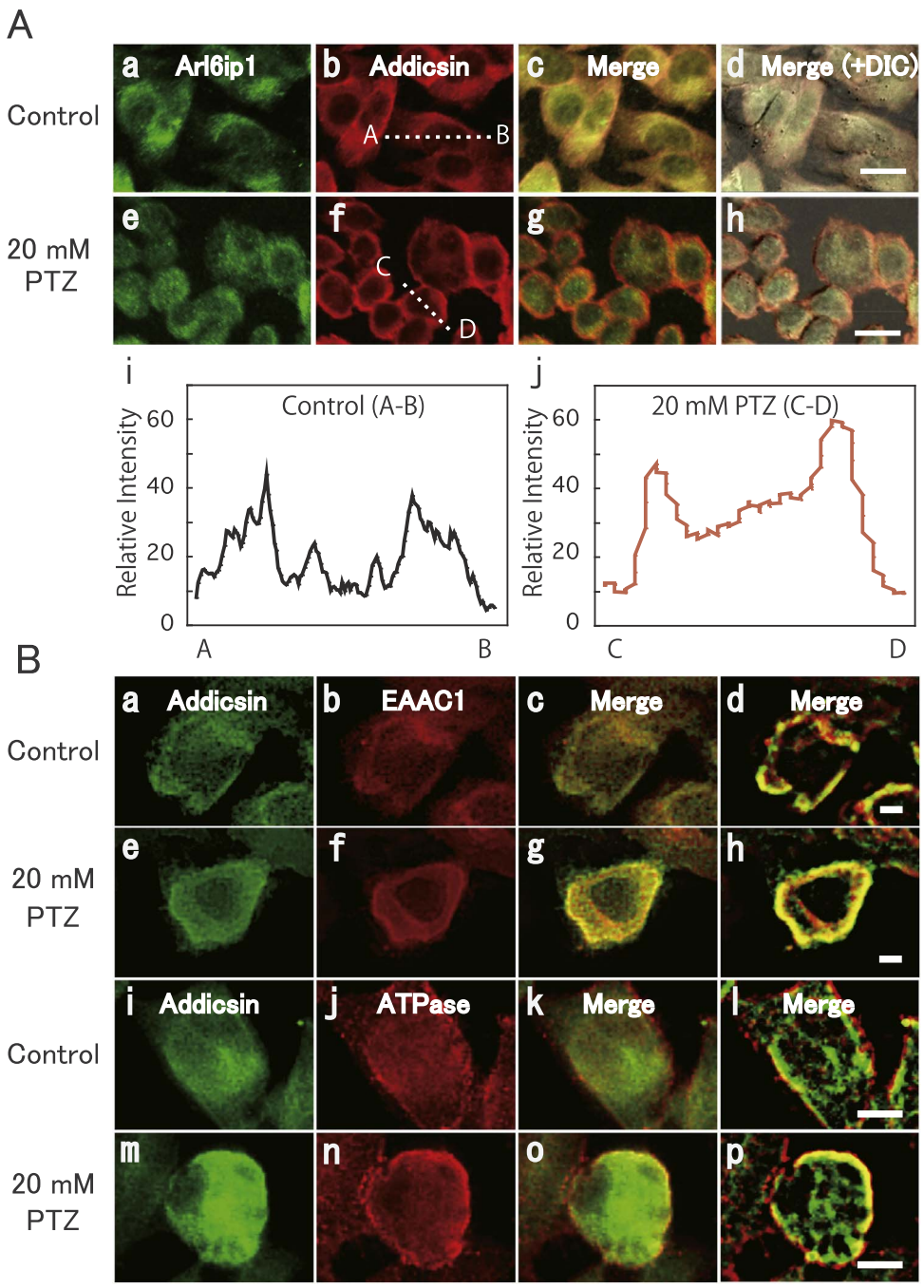

Fig. 2. Translocation of addicsin from ER to plasma membrane upon PTZ exposure. (A) (Aa–Ah) Double fluorescent immunostaining analysis of addicsin protein in NG108-15 cells after 20 mM PTZ exposure for 24 h. Both addicsin-IR (red) and Arl6ip1-IR (green) were observed using a confocal scanning microscope. Representative staining images are shown (Ai and Aj). The panels Ad and Ah showed the combined images of the double-fluorescent images and the differential interference contrast (DIC) images. Plot profile analysis using Image J at the dashed line between A and B or C and D. The PTZ exposure induced a change of addicsin localization from the ER to the plasma membrane. (B) Change of addicsin localization from the ER to the plasma membrane upon PTZ exposure. Addicsin (green) predominantly co-localized with EAAC1 (red) and Na^+/K^+ATPase at the plasma membrane (merge; yellow). To clarify the localization of addicsin at the plasma membrane, panels Bd, Bh, Bi, and Bp show the highlighted fluorescent intensity of panels Bc, Bg, Bk, and Bo, respectively. Scale bar corresponds to 20 μm in (A) and 10 μm in (B).

3. Results

3.1. Expression profile of addicsin in NG108-15 cells

We first examined the addicsin expression profile in NG108-15 cells. RT-PCR analysis showed that addicsin transcript was expressed in NG108-15 cells as well as in 293 T cells, a human embryonic kidney cell line (Fig. 1A). Western blot analysis revealed that anti-addicsin antibody exclusively recognized a single 23-kDa band in whole-cell lysates of NG108-15, which is consistent with the calculated molecular weight of addicsin, in agreement with our previous report (Fig. 1B) [2,5,16]. The expression levels of addicsin protein were increased by 20 mM PTZ for 24 h compared with that of addicsin under normal conditions (Fig. 1B). Furthermore, fluorescent immunocytochemical analysis demonstrated that addicsin immunoreactivity (addicsin-IR) was predominantly localized at the plasma membrane upon PTZ exposure for 24 h and was significantly increased 7.1-fold (Fig. 1C). These effects were significantly recognized within 1 h after exposure to 10 mM PTZ and promoted in a time-dependent manner (Fig. 1D). These findings suggest that PTZ induces the translocation of addicsin from the ER to the plasma membrane and also enhances its expression level in NG108-15 cells.

3.2. PTZ-induced addicsin translocation from ER to plasma membrane

Next, we investigated the effect of PTZ exposure on intracellular addicsin localization in NG108-15 cells by double immunocytochemical analysis using Arl6ip1 (Fig. 2A). As Arl6ip1 is an ER-integrated protein that associates with addicsin under normal conditions [5,17], it is suitable for examining the change of intracellular addicsin localization upon PTZ exposure. Indeed, addicsin immunoreactivity (addicsin-IR) was shown to be predominantly co-localized with Arl6ip1

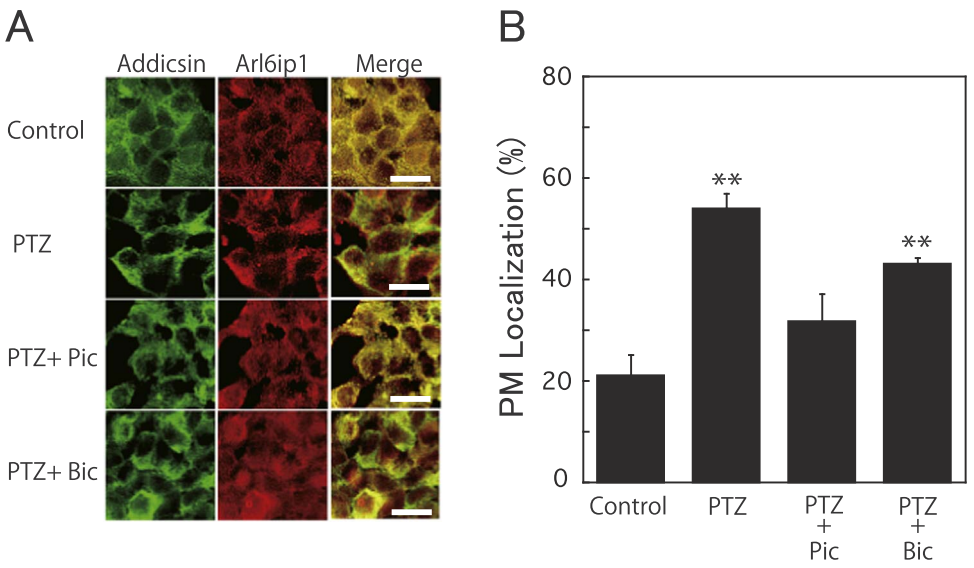

Fig. 3. Effect of GABA antagonists on PTZ-induced addicsin translocation. (A) Inhibition of PTZ-induced addicsin translocation by $GABA_A$ antagonist. The addicsin translocation was examined by double fluorescent immunostaining using anti-addicsin antibody and anti-Arl6ip1 antibody. Cells were co-incubated with 50 μM picrotoxin, a non-competitive $GABA_A$-receptor antagonist that bind the picrotoxin binding site on its receptor, or 30 μM bicuculline, a competitive $GABA_A$-receptor antagonist that recognize GABA specific binding site on its receptor, in addition to 20 mM PTZ. (B) The proportion of cells in which addicsin was localized to the plasma membrane upon PTZ exposure was evaluated by image analysis using Image J. Data are mean ± S.E.M, $n = 4$; $F_{3,\ 15} = 14.47$, $p < 0.001$; one-way ANOVA, **, $p < 0.01$ vs. Control group. Scale bar corresponds to 20 μm in (A).

immunoreactivity (Arl6ip1-IR) in the ER under normal conditions (Fig. 2Aa–Ad). On the other hand, addicsin-IR was significantly transferred from the ER to the plasma membrane regardless of the lack of a change of Arl6ip1-IR localization pattern upon exposure to 20 mM PTZ (Fig. 2Ae–Ah). Plot profile analysis using Image J showed a drastic increase in addicsin fluorescent intensity around the plasma membrane upon treatment with 20 mM PTZ (Fig. 2Ai and Aj). Furthermore, 20 mM PTZ exposure enhanced the co-localization of addicsin-IR with EAAC1-IR (Fig. 2Ba–Bh) and Na^+/K^+ATPase-IR (Fig. 2Bi–Bp).

3.3. Effect of GABA antagonists on PTZ-induced addicsin translocation

To clarify the cell signal cascade behind the PTZ-induced change in addicsin localization from the ER to the plasma membrane, double fluorescence labeling analysis was carried out using several GABA receptor antagonists in NG108-15 cells. Microscopic observations showed that addicsin-IR localized at the plasma membrane increased significantly upon 20 mM PTZ treatment. In contrast, it returned to the control level upon the co-administration of 20 mM PTZ with 50 μM picrotoxin, a non-competitive $GABA_A$ receptor antagonist, but not 30 μM bicuculline, a competitive $GABA_A$ receptor antagonist (Fig. 3A and B). These findings suggest that PTZ effect is independent of GABA binding to its specific site on $GABA_A$ receptor and that $GABA_A$ receptor-mediated cell signaling mainly regulates addicsin localization in NG108-15 cells.

3.4. Physiological significance of PTZ-induced addicsin translocation

Addicsin negatively modulates EAAC1 and participates in the oxidative stress-induced cell damage by the decrease of GSH synthesis via the inhibition of EAAC1-mediated cysteine uptake. Hence, to confirm the plasma membrane localization of addicsin by PTZ exposure, we performed both LDH assay and DPPH radical-scavenging assay. The LDH assay demonstrated that PTZ-induced cytotoxicity was increased in a PTZ dose-dependent manner (Fig. 4A), but was returned to the control level by the co-administration of picrotoxin, a $GABA_A$ antagonist, also in a dose-dependent manner (Fig. 4B). In addition, the DPPH assay indicated that the radical-scavenging activity was significantly inhibited in a PTZ dose-dependent manner, which was almost completely recovered by the co-administration of 100 μM picrotoxin (Fig. 4C), but not 30 μM bicuculline (Fig. 4D). These findings demonstrate that PTZ exposure may induce the association of addicsin with EAAC1 at the plasma membrane, which leads to a decrease in antioxidant ability by negatively modulating the EAAC1-mediated GSH synthesis.

4. Discussion

In this study, we found that addicsin changes its localization from the ER to the plasma membrane upon PTZ exposure (Figs. 1 and 2). Arl6ip1 is an ER-integrated membrane protein that acts as an apoptosis regulatory factor [18]. As shown in our previous report, addicsin forms a hetero-complex with Arl6ip1 via its hydrophobic region at amino acids 103–117 and is predominantly localized at the ER under normal conditions [5]. We observed that PTZ exposure dramatically changed the addicsin-IR pattern, although the Arl6ip1-IR pattern did not change (Fig. 2A), and promoted the co-localization of addicsin with EAAC1 and Na^+/K^+ ATPase, markers of the plasma membrane. These findings suggest that addicsin changes its localization from the ER to the plasma membrane. Furthermore, addicsin localization remarkably moved from the ER to the plasma membrane within 1 h after PTZ exposure (Fig. 1D), indicating that addicsin at the plasma membrane is translocated from the ER, but not is accumulated by PTZ-induced protein synthesis. Furthermore, our double fluorescent immunostaining analysis demonstrated that this translocation is almost completely blocked by the co-administration of 50 μM picrotoxin, a non-competitive $GABA_A$ receptor antagonist, but not that of 30 μM bicuculline, a competitive $GABA_A$-receptor antagonist (Fig. 3). In LDH assay, PTZ-induced cytotoxicity was not returned to the control level by the co-administration of 30 μM bicuculine (data not shown, 150.9 ± 4.5% of control, $n = 6$, One-way ANOVA, $p < 0.001$ vs. control group). Furthermore, PTZ-induced radical-scavenging activity was not blocked by co-administration of 30 μM bicuculine in DPPH assay (Fig. 4D). These results indicated that PTZ-induced addicsin translocation is a physiological event downstream of $GABA_A$ receptor signaling mediated through the specific picrotoxin binding site on its receptor.

The LDH assay and the DPPH radical scavenging assay indicated that PTZ-induced addicsin translocation is strongly linked to an increase of cytotoxicity and a decrease of radical-scavenging activity (Fig. 4). These findings suggest that the translocation of addicsin to the plasma membrane may cause inhibition of GSH synthesis by the association with EAAC1, which leads to damage to the intracellular redox system. However, Annexin V staining analysis showed that the cells treated with 20 mM PTZ for 24 h exhibited no Annexin V signals (data not shown), suggesting that PTZ exposure does not lead to cell death because Annexin V is an indicator of intermediate stages of apoptosis. Moreover, addicsin expression levels at 24 h after PTZ exposure were significantly upregulated (Fig. 1B and C). Thus, the PTZ-induced

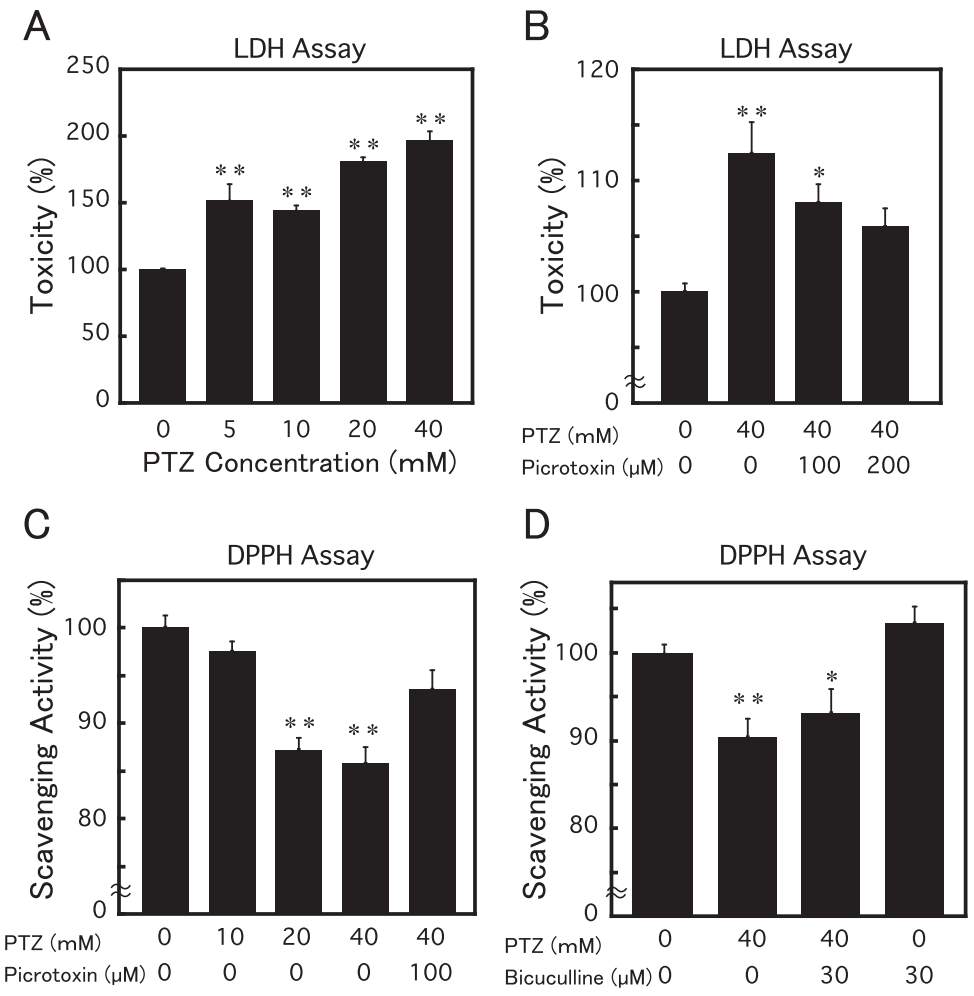

Fig. 4. Physiological significance of PTZ-induced addicsin translocation. (A) Dose-dependent effect of PTZ on cytotoxicity in NG108-15 cells. LDH assay demonstrated that PTZ increased cytotoxicity in NG108-15 cells in a dose-dependent manner. Data are mean ± S.E.M, $n = 6$; $F_{4, 29} = 32.65$, $p < 0.001$; one-way ANOVA, **, $p < 0.01$ vs. Control (0 mM PTZ) group. (B) The inhibition of PTZ-induced cytotoxicity of NG108-15 cells by the co-administration of picrotoxin, a $GABA_A$ antagonist. LDH assay showed the recovery of PTZ-induced cytotoxicity in a picrotoxin dose-dependent manner. Data are mean ± S.E.M, $n = 6$; $F_{3, 23} = 7.14$, $p < 0.01$; one-way ANOVA, *, $p < 0.05$ vs. Control (0 mM PTZ) group; **, $p < 0.01$ vs. Control (0 mM PTZ) group. (C) Dose-dependent effect of PTZ on the scavenging activity in NG108-15 cells. DPPH assay revealed the decrease of radical-scavenging activity in a PTZ dose-dependent manner. Data are mean ± S.E.M, $n = 6$; $F_{4, 24} = 13.81$, $p < 0.001$; one-way ANOVA, **, $p < 0.01$ vs. Control (0 mM PTZ) group. (D) No effect of bicuculline on the radical-scavenging activity in NG108-15 cells. DPPH assay revealed no recovery of PTZ-induced radical scavenging activity by co-administration of bicuculline. Data are mean ± S.E.M, $n = 5$; $F_{4, 19} = 6.85$, $p < 0.001$; one-way ANOVA, **, $p < 0.01$ vs. Control (0 mM PTZ) group. *, $p < 0.05$ vs. Control (0 mM PTZ) group.

addicsin translocation may act as a trigger for the activation of cell death signaling that is controlled by the homeostatic function for preventing cell death.

In summary, we found that addicsin changed its localization from the ER to the plasma membrane upon PTZ exposure. Furthermore, this change was accompanied by a decrease of radical-scavenging activity and an increase of cytotoxicity. Thus, addicsin may participate in physiological functions by changing its intracellular localization to exchange its binding partner in epilepsy.

Acknowledgements

This work was supported by research grants from the National Institute of Advanced Industrial Science and Technology (M.J. Ikemoto) and by Grant-in Aid for Scientific Research (C26450118) from the Ministry of Education, Culture, Sports, Science, and Technology of Japan (P-C. Wang).

Appendix A. Transparency document

Transparency document associated with this article can be found in the online version at http://dx.doi.org/10.1016/j.bbrep.2017.06.008.

References

[1] M. Ikemoto, M. Takita, T. Imamura, K. Inoue, Increased sensitivity to the stimulant effects of morphine conferred by anti-adhesive glycoprotein SPARC in amygdala, Nat. Med 6 (2000) 910–915.
[2] M.J. Ikemoto, K. Inoue, S. Akiduki, T. Osugi, T. Imamura, N. Ishida, M. Ohtomi, Identification of addicsin/GTRAP3-18 as a chronic morphine-augmented gene in amygdala, Neuroreport 13 (2002) 2079–2084.
[3] M.J. Ikemoto, T. Arano, Modulation of EAAC1-mediated Glutamate Uptake by Addicsin, in: D. Ekinci (Ed.), Biochemistry, InTech, Rijeka, 2011, pp. 341–364.
[4] C.I. Lin, I. Orlov, A.M. Ruggiero, M. Dykes-Hoberg, A. Lee, M. Jackson, J.D. Rothstein, Modulation of the neuronal glutamate transporter EAAC1 by the interacting protein GTRAP3-18, Nature 410 (2001) 84–88.
[5] S. Akiduki, M.J. Ikemoto, Modulation of the neural glutamate transporter EAAC1 by the addicsin-interacting protein ARL6IP1, J. Biol. Chem. 283 (2008) 31323–31332.
[6] T. Arano, S. Fujisaki, M.J. Ikemoto, Identification of tomoregulin-1 as a novel addicsin-associated factor, Neurochem. Int. 71 (2014) 22–35.
[7] K. Aoyama, T. Nakaki, Inhibition of GTRAP3-18 May Increase Neuroprotective Glutathione (GSH) Synthesis, Int. J. Mol. Sci. 13 (2012) 12017–12035.
[8] M. Watabe, K. Aoyama, T. Nakaki, Regulation of glutathione synthesis via interaction between glutamate transport-associated protein 3-18 (GTRAP3-18) and excitatory amino acid carrier-1 (EAAC1) at plasma membrane, Mol. Pharmacol. 72 (2007) 1103–1110.
[9] M. Watabe, K. Aoyama, T. Nakaki, A dominant role of GTRAP3-18 in neuronal glutathione synthesis, J. Neurosci. 28 (2008) 9404–9413.
[10] U. Ueda, T. Doi, A. Nakajima, J. Tokumaru, N. Tsuru, Y. Ishida, The functional role of glutamate transporter associated protein (GTRAP3-18) in the epileptogenesis induced by PTZ-kindling, Annu. Report. Jpn. Epilepsy Res. Found. 17 (2006) 33–40.
[11] J.P. Sepkuty, A.S. Cohen, C. Eccles, A. Rafiq, K. Behar, R. Ganel, D.A. Coulter, J.D. Rothstein, A neuronal glutamate transporter contributes to neurotransmitter GABA synthesis and epilepsy, J. Neurosci. 22 (2002) 6372–6379.
[12] J.D. Rothstein, L. Martin, A.I. Levey, M. Dykes-Hoberg, L. Jin, D. Wu, N. Nash, R.W. Kuncl, Localization of neuronal and glial glutamate transporters, Neuron 13 (1994) 713–725.
[13] Y. Nunez-Figueredo, J. Ramirez-Sanchez, R. Delgado-Hernandez, M. Porto-Verdecia, E. Ochoa-Rodriguez, Y. Verdecia-Reyes, J. Marin-Prida, M. Gonzalez-Durruthy, S.A. Uyemura, F.P. Rodrigues, C. Curti, D.O. Souza, G.L. Pardo-Andreu, JM-20, a novel benzodiazepine-dihydropyridine hybrid molecule, protects mitochondria and prevents ischemic insult-mediated neural cell death in vitro, Eur. J. Pharmacol. 726 (2014) 57–65.
[14] K.K. Mishra, R.S. Pal, R. Arunkumar, C. Chandrashekara, S.K. Jain, J.C. Bhatt, Antioxidant properties of different edible mushroom species and increased bioconversion efficiency of Pleurotus eryngii using locally available casing materials, Food Chem. 138 (2013) 1557–1563.
[15] C.A. Schneider, W.S. Rasband, K.W. Eliceiri, NIH Image to ImageJ: 25 years of

image analysis, Nat. Methods 9 (2012) 671–675.
[16] S. Akiduki, T. Ochiishi, M.J. Ikemoto, Neural localization of addicsin in mouse brain, Neurosci. Lett. 426 (2007) 149–154.
[17] M. Kuroda, S. Funasaki, T. Saitoh, Y. Sasazawa, S. Nishiyama, K. Umezawa, S. Simizu, Determination of topological structure of ARL6ip1 in cells: identification of the essential binding region of ARL6ip1 for conophylline, FEBS Lett. 587 (2013) 3656–3660.
[18] H.M. Lui, J. Chen, L. Wang, L. Naumovski, ARMER, apoptotic regulator in the membrane of the endoplasmic reticulum, a novel inhibitor of apoptosis, Mol. Cancer Res. 1 (2003) 508–518.